Pastor Soriano, JV.; García Oliver, JM.; García Martínez, A.; Mico Reche, C.; Durret, R. (2013). A spectroscopy study of gasoline partially premixed compression ignition spark assisted combustion. Applied Energy. 104:568-575. doi:10.1016/j.apenergy.2012.11.030.

# A Spectroscopy Study of Gasoline Partially Premixed Compression Ignition Spark Assisted Combustion

J.V. Pastor[1], J. M. García-Oliver[1], A. García[1*], C. Micó[1] and R. Durrett[2]

[1]CMT- Motores Térmicos - Universitat Politécnica de Valencia, Camino de Vera s/n 46022 Valencia - SPAIN

[2]Diesel Engine Systems Group - Propulsion Systems Research Lab GM R&D Center, MC: 480-106-252, 30500 Mound Rd, Warren, MI 48090-905

**(*) CORRESPONDING AUTHOR:**

Dr. Antonio Garcia: angarma8@mot.upv.es

Telephone: +34 963879659

Fax: +34 963877659

## ABSTRACT

Nowadays many research efforts are focused on the study and development of new combustion modes, mainly based on the use of locally lean air-fuel mixtures. This characteristic, combined with exhaust gas recirculation, provides low combustion temperatures that reduces pollutant formation and increases efficiency. However these combustion concepts have some drawbacks, related to combustion phasing control, which must be overcome. In this way, the use of a spark plug has shown to be a good solution to improve phasing control in combination with lean low temperature combustion. Its performance is well reported on bibliography, however phenomena involving the combustion process are not completely described. The aim of the present work is to develop a detailed description of the spark assisted compression ignition mode by means of application of UV-Visible spectrometry, in order to improve insight on the combustion process.

Tests have been performed in an optical engine by means of broadband radiation imaging and emission spectrometry. The engine hardware is typical of a compression ignition passenger car application. Gasoline was used as the fuel due to its low reactivity. Combining broadband luminosity images with pressure- derived heat- release rate and UV- Visible Spectra, it was possible to identify different stages of the combustion reaction. After the spark discharge, a first flame kernel appears and starts growing as a premixed flame front, characterized by a low and constant heat-release rate in combination with the presence of remarkable OH radical radiation. Heat release increases temperature and pressure inside the combustion chamber, which causes the auto-ignition of the rest of the unburned mixture. This second stage is characterized by a more pronounced rate of heat release and a faster propagation of the reactions through the combustion chamber. Moreover, the measured UV-Visible spectra show some differences in comparison with the other stages. The relative intensities in of spectra from different combustion radicals have also been related to the different combustion phases.

## KEYWORDS:

PPC, Spark assistance, Gasoline fuel, Optical Investigation, Combustion description

## HIGHLIGHTS

- PPC combustion combined with spark assistance and gasoline fuel on a CI engine
- Chemiluminescence of different chemical species describes the progress of combustion reaction.
- Spectra of a novel combustion mode under SACI conditions is described.
- UV-Visible spectrometry, high speed imaging and pressure diagnostic were employed for analysis.

## NOMENCLATURE

| | |
|---|---|
| *CI* | Compression Ignition |
| *ICE* | Internal combustion engine |
| *EGR* | Exhaust gas recirculation |
| *PPC* | Partially premixed combustion |
| *SACI* | Spark assisted compression ignition |
| *ROHR* | Rate of heat release |
| *CAD* | Crankangle degree |
| *ACV* | Apparent combustion velocity |

## 1. INTRODUCTION

Nowadays the automotive scientific community focuses part of their efforts on the investigation of new combustion modes [[1]] with the aim of reducing fuel consumption and emissions in CI (Compression Ignition) diesel engines [2, [2]]. These modes are mainly characterized by taking place under homogeneous locally lean conditions which, combined with high exhaust gas recirculation rates, provide low combustion temperatures. As a consequence, NOx and soot formation are reduced while fuel consumption and efficiency improve [4].

In spite of their benefits, these combustion concepts present some challenges that must be overcome before their practical implementation in ICEs. The main limitation is obtaining a proper combustion phasing and control over a wide range of engine load and speed. Highly-premixed combustion modes in CI engines are dominated by chemical kinetics, which are directly dependent on temperature and chemical composition of the mixture. As a consequence, achieving the proper ignition conditions requires both adequate mixing and temperature of the charge. To solve this problem, different strategies have been proposed [5-7]. Temperature can be controlled by intake air heating or modifying the compression ratio. Other strategies like control of EGR rate [27] or the amount of trapped combustion gases also modifies mixture composition. Multiple injection strategies and combinations of different fuels have also been investigated. However, the majority of the techniques mentioned cannot provide precise control over the combustion phasing, since they require time scales too large to achieve cycle-by-cycle control.

All previous actions try to compensate the high chemical reactivity of the diesel fuel that does not provide enough mixing time before the start of combustion. Thus, recent studies have tried to overcome these disadvantages by using fuels with different reactivities. PPC (Partially Premixed Combustion) is a novel combustion strategy with the main characteristic being the use of a low reactivity fuel [[7], [8], [9]]. This combustion mode is in transition between normal diffusion combustion in CI engines and Premixed Charge Compression Ignition (PCCI). It allows a high degree of fuel-air mixing before ignition but the charge is not completely homogeneous [[10], 12]. Nevertheless,

while all these solutions provide some control of the combustion phasing, they still cannot deliver the required cycle-to-cycle control capability of these partial or fully premixed combustion processes. Moreover, when a very low reactivity fuel is used [13, 28], it is not possible to achieve stable engine operation for light and mid load conditions.

Spark assisted combustion phasing and control has been investigated for controlled auto-ignition (CAI) implementation in port fuel injection SI engines. The spark plug has been used to supply the necessary energy for achieving a controlled auto-ignition process with a method referred to as Spark Assisted Compression Ignition (SACI). In this mode, the combustion process is composed of a first growth of a reaction kernel, due to the energy supplied by the spark, which leads to the start of a propagating flame. The flame propagation combustion consumes part of the fuel, releasing energy that increases the mixture temperature and provokes its auto-ignition. Since flame propagation is generally slower than auto-ignition, this mechanism reduces the overall heat release rate. Previous experimental work using spark ignition engine architecture [14, 15] and moderate reactivity fuels suggests that this method can provide good combustion phasing while the response time is short enough for cycle-by-cycle application[16, 17].

In the present work, combustion phasing control by means of a spark plug ignition system is integrated on a CI engine working in partially a premixed combustion (PPC) mode, when a very low reactivity fuel is used. On the one hand, the spark plug offers a cycle-to-cycle control over PPC regardless of thermodynamic conditions. On the other hand the CI engine, which is not common in the SACI literature, allows to overcome some previously reported problems related to the use of high octane fuels, like misfiring under light load engine conditions. Experiments have been performed in an optical engine, with a diesel-like compression ratio and geometry, equipped with a common rail injection system enabling high-pressure injection, EGR and temperature control. Moreover, the experimental work was carried out using gasoline, because of its low reactivity. Since the investigation was performed in an optical engine, different tools were combined in the study: in-cylinder pressure analysis, combustion broadband imaging and emission spectrometry. The latter has been proven as a powerful tool for analysis of new combustion modes, so it is used to develop a detailed description

and improve the existing knowledge about the phenomenology of the gasoline partially premixed combustion compression ignition mode with spark assistance. Therefore, the main objective of the work is the improvement of the fundamental understanding of this combustion process.

## 2. EXPERIMENTAL TOOLS AND MEASUREMENT PROCEDURE

### 2.1. Engine

The experimental work was performed at a low load-operation mode on a 4-stroke DI diesel single cylinder optical engine (Fig.1) with the specifications listed in Table 1. It is equipped with an elongated piston and a cylindrical bowl, with dimensions of 45 x 18 mm (diameter x depth), allowing optical access to the combustion chamber through a sapphire window located at its bottom. Below the piston bowl an elliptical UV mirror is placed at 45º, aligned with the piston axis.

The cylinder head is a modified 2.2 HSDI 4 valve diesel cylinder head. One of the exhaust valves was removed in order to install a spark plug. This modification does not strongly affect air management, due to the low operating engine speed and the skip fire methodology used in this work. The engine is equipped with a conventional common rail injection system. The injector is positioned at the center of the combustion chamber and oriented so that one of the jets passes through the spark electrodes. Tests were conducted in skip-fire mode to prevent fouling of the optical access and minimize thermal engine gradients; thus, only one injection is performed every 30 cycles. This methodology ensures repetitive engine conditions between fired cycles.

In-cylinder pressure is measured, and thermodynamic analysis is performed with a one-zone model CALMEC [20, 22]. This diagnosis tool uses the measured in-cylinder pressure as the main input and other engine parameters as boundary conditions of the test. The model's main result is the Rate

of Heat Release (ROHR). Time resolution for these variables depends on the crank angle encoder configuration (0.2 CAD).

All the tests were carried out under the same engine conditions. Engine speed was set to 750 rpm. This low regime offers long cycle and combustion duration, which are optimum conditions to check the viability of the combustion mode. Intake air temperature and pressure were set to 303 K and 1.6 bar respectively. This intake pressure, which is a common value for this engine under HCCI combustion conditions, has been selected in order to avoid wall impigment. O2 concentration inside combustion chamber is controlled using a synthetic EGR system, where EGR gases are substituted only by N2. For this study, XO2 was fixed at 18%. Fuel was commercial gasoline with 95 octane number (RON) and 765 kg/m3 density. The start of injection was located 19 crank angle degrees before top dead center, injecting 20.6 mg of fuel per cycle, which results in an average 0.35 equivalence ratio. Due to the low reactivity of the fuel, no ignition occurs under these operating conditions when no spark plug discharge is performed. The spark discharge was located at -10 CAD, coinciding with the end of injection, while the local air-fuel mixture around the spark plug is still rich enough and thermodynamic conditions are adequate for ignition. To enable an adequate mixture preparation in the spark plug zone within the required time scales, injection pressure was set to 600 bar. This pressure is higher than the usual range offered by commercial direct injection gasoline systems, so a common rail Bosch-Piezo system was used.

## 2.2. Optical Apparatus

Digital imaging and spectroscopic analysis in the UV-Visible range were performed. Light emitted by the combustion process is reflected by the UV Mirror and guided to both a high speed camera and a spectrograph. The optical set-up is shown in Fig. 2.

In order to register temporal and spatial evolution of broadband radiation from the combustion process a Photron Fastcam Ultima APX camera was employed. This High Speed CMOS camera was used to record at 6000 fps with a 512 x 512 pixels resolution. The exposure time was fixed at

166 166.7 μs (approx. 0.75 CAD), ensuring a good dynamic range although soot emission could saturate
167 the images. The lens used is a Zeiss 100mm f/2 ZF Makro-Planar, keeping the aperture constant for all
168 the tests. This element restricts the bandwidth of light recorded to the visible range. The whole optical
169 system provides an effective resolution of 0.17mm/pixel for the images.

170 A Jovin Yvon Horiba Triax 180 spectrograph was used to decompose the light emitted by
171 combustion in the UV-Visible range, which was coupled with a LaVisionDynamight intensified CCD
172 camera. A grating with 300 groove/mm was used which, combined with the 512 x 512 pixels of the
173 ICCD camera, allows detecting a wavelength bandwidth of 170 nm. Two different configurations were
174 chosen, the first one with the grating centered at 350 nm (265-435 nm) for the UV range and the other
175 one centered at 450 nm (365 – 535 nm) for the visible range. The entrance slit width was set to 0.3
176 mm and the exposure time of the ICCD camera was 500 μs (approx. 2.25 CAD). A UV-Lens (Ø25.4 - 100
177 mm focal length) was used to focus the light inside the spectrograph.

178

## 179 2.3. Image Processing

180 A processing routine was applied to the high speed camera images, to obtain numerical
181 information about the size and shape of the combustion area for further analysis. Each image was
182 binarized considering a fixed threshold value, so pixels corresponding to the flame (higher intensity
183 than threshold) are assigned a value of 1, while pixels of the background (lower intensity than
184 threshold) are assigned a value of 0. Flame area is defined as the addition of all pixels set to 1. In a
185 second step, the contour of the flame was obtained from the binarized image. Fig. 3 presents an
186 example of the different processing steps.

187 For the analysis of the flame propagation velocity, a geometrical magnitude was defined. Fig. 8
188 shows that flame shape changes during the combustion cycle. The first steps of the reaction are
189 characterized by a geometrically continuous flame, there is a middle stage when the flame shrinks and
190 breaks into different parts. In order to characterize this behavior, the time derivative of the ratio

191 between flame area and contour length is obtained. In this way, not only a change of flame area is
192 characterized but also its fragmentation due to a reaction slowdown. From now on, this magnitude
193 will be named as apparent combustion velocity (ACV).

194

## 195 3. RESULTS AND DISCUSSION

### 196 3.1. Analysis of combustion repeatability

197 In the subsequent sections, the description of the SACI combustion sequence will be presented in
198 terms of a single cycle results (Figs. 8 and 9). This approach will be justified in the present section,
199 where cycle-to-cycle scattering will be evaluated to show that combustion is repeatable.

200 On the one hand, Fig 4 shows a comparison between the cycle-to-cycle variation of the rate of heat
201 release (shadowed area) and the cycle that will be used to describe combustion events (thick black
202 curve). There is consistency among the entire set of cycles and the one chosen to analyze within the
203 article, so this cycle should be considered as representative of the combustion process. A more
204 detailed analysis is included in the Figure 5. In order to represent the combustion phasing variability,
205 the starting and end point of the two main phases of the combustion process (premixed and
206 autoignition length) have been obtained from the RoHR of each cycle. Moreover, the maximum RoHR
207 value at each of these phases has been registered. SoC refers to the start of combustion, while End of
208 Premixed and Autoignition Phase correspond to the ending CAD of different combustion phases.
209 Variability of both combustion phasing and heat released during the combustion process are reduced.
210 Thereby, this confirms that all the cycles that conforms this work have a very similar combustion
211 evolution along the engine cycle compared to the reference one.

212 On the other hand, the scattering among cycles in the natural luminosity images has also been
213 analyzed. For that purpose, flame area and accumulated intensity evolution have been chosen. Fig. 6
214 and Fig. 7 show the flame area and total intensity for the 30 cycles employed on the RoHR cycle-to-
215 cycle variation study. Both figures present a grey curve and a shadowed area, which indicate the

average +- one standard deviation as calculated from the single cycles of accumulated intensity and flame area. The black curve represents the corresponding evolution for the cycle employed on the description of the combustion process. It can be seen that scattering, in both cases, is higher than the one presented for RoHR. However, the trend along combustion cycle is well defined and the one included in the subsequent sections for analysis follows the average behavior. According to these results, as well as to the information from the heat release curves, the information selected for the description of the combustion cycle is representative of engine behavior.

## 3.1. Analysis of flame radiation images

A first description of the phenomena involved in partially premixed compression ignition spark assisted combustion can be obtained from the analysis of the natural luminosity released by reaction Fig. 8 shows a crankangle resolved sequence of images of the reference combustion cycle. For brevity, only every other recorded image is shown. After the spark discharge (-10.0 CAD), a high luminosity area is observed around the spark plug (-10.3 CAD). This active site shifts towards the combustion chamber wall, and later on slightly reduces in size but it does not change in position. At -7.4 CAD, however, the luminous area is seen to have expanded, but its appearance is different: the original high intensity spot from the spark discharge still exists, but it is surrounded by a much larger compact zone with dimmer intensity. This zone seems to be expanding to the rest of the combustion chamber but, after -4.6 CAD, it reduces in size again, becoming less compact in appearance. This reduction phase finishes at -0.3 CAD, from which a second increase in luminous area is observed. During this phase, the luminous area progresses towards the rest of the combustion chamber, with a relatively low intensity appearance except for some locally bright spots that will be discussed below. After 7.0 CAD, the radiation zone starts to reduce again, but this time it leads to the extinction of the reaction zone.

The previous qualitative sequence can be analyzed in terms of quantitative variables derived from in-cylinder pressure and image processing as shown in Fig. 9. The evolution of the combustion area is in agreement with the previous images: spark discharge occurs at -10.0 CAD, and no large increase in

area occurs until approximately -8.0 CAD, as shown in the ACV evolution. During that interval, only the spark generated radiation occurs. From -8.0 CAD to approximately -2.0 CAD (minimum value in area after the first maximum) the phase of the compact radiation area evolution occurs. From -2.0 CAD onwards, a second combustion period occurs with the corresponding increase in area. Both phases are marked by a corresponding ACV peak. It is noticeable that all three periods can also be observed to be approximately coincident with those observed in the pressure-derived heat release rate, namely a first phase without heat release from spark timing to -9.0 CAD, a second period with a sustained heat release until -1.0 CAD, after which a third period with a noticeable peak in heat release occurs. Both differences between second and third phases in heat release values and, to a lower extent, in area and ACV, indicate that the last one is faster than the second one.

Previous analysis of quantitative parameters makes it possible to define three different stages during the combustion process. After the spark discharge, a growth of an early flame kernel takes place with negligible heat release. The kernel phase it is followed by a flame front propagation under premixed conditions. Energy released by premixed reaction causes an increase in temperature and pressure in the combustion chamber, leading to the autoignition of the rest of the mixture. The mean difference between autoignition and premixed combustion phases is the propagation rate and, as a consequence, the maximum values attained by the rate of heat release. Moreover, it can be seen that reaction is not uniform along the combustion chamber. While the premixed combustion takes place around the spark plug, the auto-ignition phenomenon extends to the whole field of view. The description obtained is consistent with the work of other authors, such as Natarajan and Tornatore [17, 23].

## 3.2. Analysis of radiation spectra

Spectral analysis is useful in order to better investigate the combustion process. In the literature, different chemical species and radicals are identified as good tracers of the stages of a hydrocarbon combustion reaction. Thus their presence changes radiation emission spectra and helps describe the evolution of the reaction.

Due to optical apparatus limitations, spectra were registered at different locations along the combustion chamber in order to obtain good spatial resolution. For the analysis, the combustion chamber was divided into nine regions of interest (Fig. 10). The size of each region is 79 x 16 pixels and had an area of 13.5 x 2.7 mm. Each region is labeled according to the horizontal (1,2,3) and vertical (T,C,B) location.

The different spectra registered during the combustion process are presented in Fig. 11 to Fig. 14. All of them correspond to central location in the chamber (1C, 2C and 3C). Results in other locations are similar. Each figure shows instantaneous spectra from two different engine cycles, as two recordings were done for each of the visible and UV wavelength ranges, however both overlap in the 400-440 nm interval. Representative timings are shown for the following combustion phenomena: 1. Spark discharge and flame kernel appearance (Fig. 11); 2. Flame growth under premixed conditions (Fig. 12); 3. Auto-ignition combustion (Fig. 13); Fig. 14 corresponds to the late combustion phase.

Fig. 11 shows spectra recorded between -10.8 and -8.5 CAD, which corresponds approximately to the interval between spark discharge and start of heat release. Light is mainly produced by the plasma generated around the spark plug terminals (zone 1C). The early interactions between excited hydrocarbon species and the air are represented by the presence of CN and NH peaks, according to the literature [23]. Moreover, the corresponding spectrum also shows two weak peaks from OH and CH emission (310 and 430 nm). Both radicals are indicators of combustion chemical reactions associated with the formation of an early flame kernel. Due to the low reaction rate during the first stage of combustion, no evidence of radical or chemical activity was detected in the rest of the combustion chamber, so no information is shown for zones 2C and 3C.

Spectra between -5.5 and -3.2 CAD correspond to the second phase of the heat release rate, where the premixed combustion reaction is progressing. These are shown in Fig. 12. The spectrum around the spark plug (1C) is similar to blackbody continuum emission. A noticeable peak of OH (310 nm) is also present. Both characteristics are a consequence of combustion occurring in fuel rich zones, with soot particles forming as a result of the accumulation of fuel close to the combustion chamber wall. At position 2C (injector), the spectra are composed only of chemiluminiscence radiation. Apart from the intense OH and CH peaks (310 and 430 nm), there is also a continuum band, starting at 270 nm and extending into the visible range. This band is usually attributed to HCO (Vayda bands, from 270 to 410 nm [24]) and HCHO radiation (Emelus bands, from 340 to 523 nm [24]). Both radicals are representative of the transition from low to high temperature combustion. According to the radiation images (Fig. 8) the reaction has reached position 2C, and therefore the recorded spectra correspond to a premixed front progressing towards the unburned mixtures. At position 3C, it was not possible to identify either radicals or chemical reactions due to the low emission levels, so spectra are not shown.

Fig. 13 shows spectra recorded during the 2 to 4.3 CAD interval, when the main auto-ignition process is underway. At location 1C the OH peak is still present, but the continuum spectrum of soot is more doubtful. Instead, spectra suggest the presence of CO as a broadband radiation between 420 and 490 nm. Both facts are consistent with the final stages of a combustion process, when soot radiation has almost disappeared, and radiation of late occurring species like CO appears [23, 24]. On the other hand, at position 2C the auto-ignited combustion is taking place. Here the recorded spectra are governed by broadband continuum emission and an intense peak of OH (310 nm). Radiation images (Fig. 8) also indicate very strong luminosity in the injector area. Both diagnostics hint at the presence of soot particulates (bright spots). This interpretation is consistent with fuel leakages observed from the injector, which ignite as a consequence of local high temperatures and, due to the lower mixing rate, form a diffusion flame. Finally, at position 3C CH and OH peaks (430 and 310 nm) can be identified, and HCO and HCHO background emission is also present. Both indicate a relatively similar emission as in location 2C, from -5.5 to -3.2 CAD, except for the stronger CH and weaker OH in this case compared

318 to -5.5 to -3.2 CAD spectra. Such differences can be explained by the different combustion regime
319 (premixed at 2C from -5.5 to -3.2 CAD vs auto-ignition at 3C from 2 to 4.3 CAD).

320 Finally, Fig. 14 shows the spectra during the interval from 5.8 to 8.0 CAD when the combustion
321 process is nearing completion. The spectrum measured at position 3C shows a weak OH peak at 310
322 nm and a broadband component, which extends to the visible range, characteristic of CO-O produced
323 from the oxidation of HCO and HCOH. This emission overlaps possible peaks of other radical like CH at
324 430 nm. This spectrum is common in the major part of the combustion chamber at this stage except
325 around the injector (2C), where the influence of fuel leakages is still present and spectra show a more
326 intense OH peak and soot broad-band emission.

327

328 ## 4. CONCLUSIONS

329 Direct visualization and spectroscopic analysis of natural radiation has been combined with the
330 analysis of the Rate of Heat Release to provide a description of the combustion process occurring in a
331 Partially Premixed Spark Assisted Compression Ignition mode using gasoline. Three different stages of
332 combustion have been identified. The process starts with the spark discharge, which produces a flame
333 kernel around the spark plug that later evolves to a premixed flame front. This premixed flame front
334 heats unburned mixture and progresses into an auto-ignition combustion that burns out the rest of
335 the charge.

336 Spectra of the combustion process change as the process evolves. During the first step of the
337 reaction (-10.8 CAD), the main radiation comes from the spark discharge and the early flame kernel
338 formed around the spark plug. The spectra is characterized by the emission due to early interaction
339 between excited hydrocarbons and air, but also by the appearance of the first reactions denoted by
340 weak peaks of OH and CH. No heat release is observed at this time.

341 As the flame front expands (-5.5 CAD), OH radiation grows and becomes very intense, and the
342 chemiluminiscence spectra also shows the presence of CH, HCO and HCHO. The resulting spectrum is

characteristic of premixed combustion, which is consistent with previously observed RoHR and flame propagation. Soot radiation is only present at the original location where ignition occurred and close to the injector, due to fuel leakages.

After the period of premixed combustion, a transition occurs to an auto-ignition phase induced by compression heating, with a more intense RoHR. Spectra show similar radicals such as HCO and HCOH, while the corresponding OH peak is weaker and CH peaks are more visible than in the previous phase, as a consequence of the change in the combustion regime.

## ACKNOWLEDGEMENTS

The authors acknowledge that part of this work was performed in the frame of project DUFUEL TRA2011-26359, funded by the Spanish Government. The authors also thank GM for technical assistance and its support in other parts of this work.

## REFERENCES

[1] Yanagihara, H., Sato, Y. and Minuta, J., “A simultaneous reduction in NOx and soot in diesel engines under a new combustion system (Uniform Bulky Combustion System -UNIBUS)”, 17th International Vienna Motor Symposium, pp 303-314, 1996.

[2] Kimura, S., Aoki, O., Ogawa, H., Muranaka, S. et al., “New Combustion Concept for Ultra-Clean and High-Efficiency Small DI Diesel Engines,” SAE Technical Paper 1999-01-3681, 1999.

[3] Akagawa, H., Miyamoto, T., Harada, A., Sasaki, S. et al., “Approaches to Solve Problems of the Premixed Lean Diesel Combustion,” SAE Technical Paper 1999-01-0183, 1999.

[4] Kimura S., Aoki S., Kitahara Y., Aiyoshizawa E. Ultra-clean combustion technology combining a low-temperature and premixed combustion concept for meeting future emission standards. SAE International, SAE 2001-01-0200, 2001.

[5] Mingfa Yao, Zhaolei Zheng, Haifeng Liu, “Progress and recent trends in homogeneous charge compression ignition (HCCI) engines”. Progress in Energy and Combustion Science, Volume 35, Issue 5, October 2009, Pages 398-437.

[6] Hanson, R. M., Kokjohn, S. L., Splitter, D. A, and Reitz, R. D. “An experimental Investigation of Fuel Reativity Controlled PCCI Combustion in a Heavy-Duty Engine” SAE international journal of engines, 2010, 3(1) 700-716.

[7] B. Keeler and P. J. Shayler, “Constraints on Fuel Injection and EGR Strategies for Diesel PCCI-Type Combustion”. SAE 2008-01-1327.

[8] Yang, J., Culp,T., and Kenney, T. Development of a gasoline engine system using HCCI technology- The concept and the test results. SAE paper 2002-1-2832.

[9] Kalghatgi, G.T., Risberg, P., and Ångström, H.-E., “Advantages of Fuels with High Resistance to Auto-Ignition in Late-Injection, Low-Temperature, Compression Ignition Combustion,” SAE Technical Paper 2006-01-3385, 2006.

[10] Kalghatgi, G.T., Risberg, P., and Ångström, H.-E., “Partially Pre-Mixed Auto-Ignition of Gasoline to Attain Low Smoke and Low NOx at High Load in a Compression Ignition Engine and Comparison with a Diesel Fuel,” SAE Technical Paper 2007-01-0006, 2007.

[11] Hildingsson, L., Kalghatgi, G., Tait, N., Johansson, B. et al., “Fuel Octane Effects in the Partially Premixed Combustion Regime in Compression Ignition Engines,” SAE Technical Paper 2009-01-2648, 2009.

[12] Sjoberg, M and Dec, J.E. “Smoothing HCCI Heat-Release using partial fuel stratification with two-stage ignition fuels”. SAE 2006-01-0629, 2006.

[13] H. Persson, A. Rémon, A. Hultqvist, B. Johansson, “Investigation of the early flame development in spark assisted HCCI Combustion Using high speed chemiluminescence Imaging”. SAE 2007-01-0212

[14] B. Johansson, “Path to High Efficiency Gasoline Engine”. DEER 2010 Lund University.

[15] H. Persson, A. Rémon, B. Johansson, “The effect of swirl on spark assisted compression ignition (SACI)” JSAE20077167, SAE 2007-01-1856 (2007).

[16] Wang, Z., Shuai, S.J., and Wang, J.-X., G-H Tian, Xinliang, Q-J Ma “Study of the effect of spark ignition on gasoline HCCI combustion”. Proceedings of the Institution of mechanical Engineers, Part D: Journal of Automobile Engineering. DOI:10.1243/09544070JAUTO151

[17] Vinod K. Natajaran, Volker Sick, David L. Reuus and Gerald Silvas, “effect of spark-ignition on combustion periods during spark assisted compression ignition”. Combustion Sci. and Tech, 181:1187-1206,2009

[18] Benajes J, López JJ, Novella R, Garcia A: “Advanced Methodology for Improving Testing Efficiency in a Single-Cylinder Research Diesel Engine”; Experimental Techniques 32:41-47, 2008.

[19] J. Benajes, R. Novella, A. Garcia, V. Domenech, “ An investigation on mixing and autoignition using diesel and gasoline in a direct injection compression ignition engine operating in PCCI combustion conditions”. SAE Int. J. Engines August 2011 4:2590-2602; doi:10.42712011-37-0008

[20] Payri F., Olmeda P., Martín J. and García A. “A complete 0D thermodynamic predictive model for direct injection diesel engines”, Applied Energy. Vol 88, issue 12, pp 4632–4641, 2011.

[21] J.V. Pastor, J.M. Garcia-Oliver, J.M. Pastor, J.G. Ramirez-Hernandez, “Ignition and combustion development for high speed direct injection diesel engines under low temperature cold start conditions”. Fuel (2011), doi:10.1016/j.fuel.2011.01.008

412 [22] Payri F, Molina S, Martín J and Armas O: “Influence of measurement errors and estimated
413 parameters on combustion diagnosis”, Applied Thermal Engineering Vol 26 Nº 2-3 pp 226–
414 236, 2006.

415 [23] Tornatore C., Sementa P., and Merola S.S.: “Optical Investigations of the early combustion
416 phase in spark ignition boosted engines”, Proceedings of the Institution of Mechanical
417 Engineers, Part D: Journal of Automobile Engineering, Vol 225; 2011.

418 [24] Gaydon A.G., The spectroscopy of flame, Chapman and Hall, London, UK, 1957.

419 [25] Mancaruso E., Vaglieco B. M.: “Spectroscopic measurements of premixed combustion in
420 diesel engine”, Fuel Vol. 90, 511-520, 2011.

421 [26] Kim B., Kaneko M., Ikeda Y., Nakajima T.: “Detailed spectral analysis of the process of HCCI
422 combustion”, Proceedings of the Combustion Institute, Vol. 29, 671-677, 2002.

423 [27] Singh A.P., Agarwal A.K. “Combustion characteristics of diesel HCCI engine: An experimental
424 investigation using external mixture formation technique”, Applied Energy, 2012.

425 [28] Yang D.-B, Wang Z., Wang J.-X., Shuai S.-J. “Experimental study of fuel stratification for HCCI
426 high load extension” Applied Energy, Vol. 88, issue 9, pp 2949 – 2954, 2011.

427 [29] Mancaruso E., Vaglieco B.M., “Premixed combustion of GTL and RME fuels in a single cylinder
428 research engine” Applied Energy, Vol. 91, issue 1, pp. 385-394, 2012

429 [30] Hwang W, Dec J., Sjöberg M., “Spectroscopic and chemical-kinetic analysis of the phases of
430 HCCI autoignition and combustion for single- and two-stage ignition fuels” Combustion and
431 Flame, Vol. 154, pp 387 – 409, 2008

432

433 Figure 1

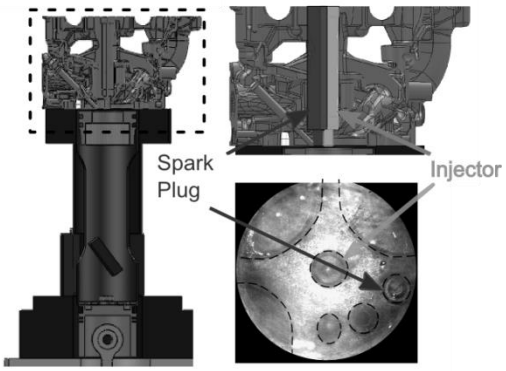


434

435 **Fig. 1 – Sketch of the single cylinder optical engine and the**
436 **modified cylinder head.**

437

438 Figure 2

439

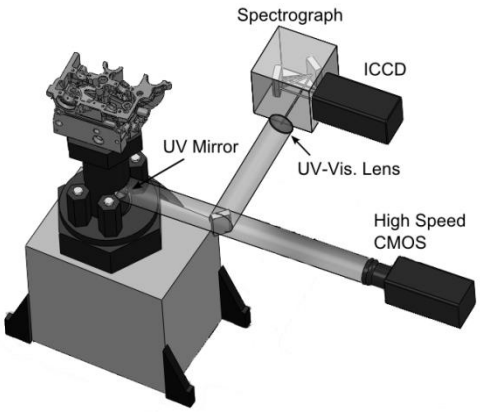


440

441 **Fig. 2 – Optical set-up scheme for registering natural**
442 **radiation from the combustion reaction**

443

444 Figure 3

445

446 **Fig. 3 – Scheme of processing steps. From left to right:**
447 **original image, binary image of the flame area and**
448 **binary image of the flame contour**

449

450 Figure 4

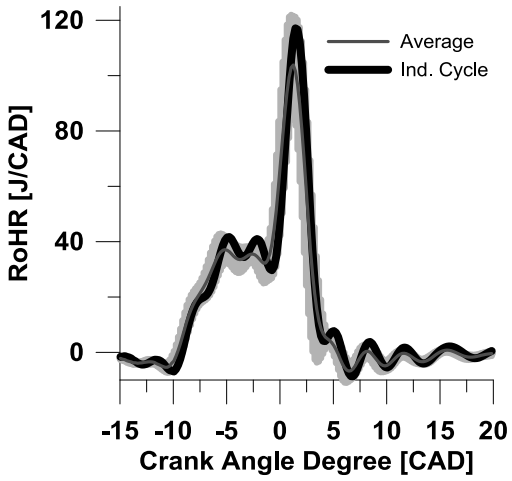


451

452 **Fig. 4 – RoHR dispersion for 30 SACI cycles. The shadowed**
453 **area represents mean RoHR ± std. deviation. Thick black**
454 **curve represents cycle employed on result discussion.**

455

456 Figure 5

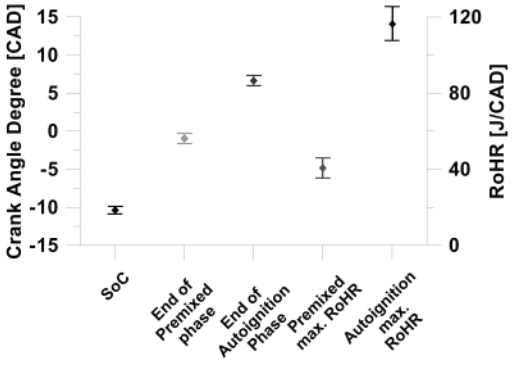


457

458 **Fig. 5 – Dispersion of two main combustion phases, considering**
459 **both phasing and maximum heat released.**

460

461

462

463

464

465

466

467

468 Figure 6

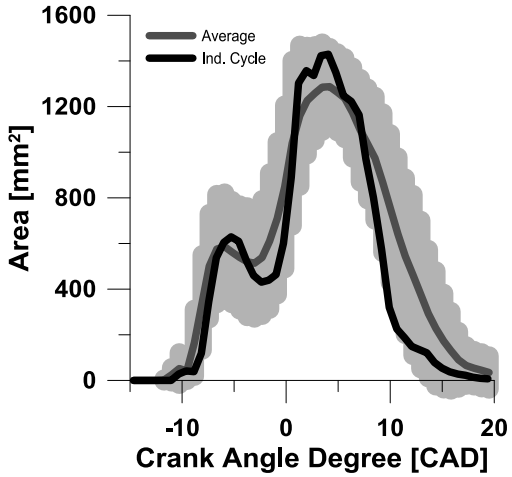


469

470 **Fig. 6 – Flame area dispersion for 30 SACI cycles. The shadowed**
471 **area represents mean Flame area ± std. deviation. Thick black**
472 **curve represents cycle employed on result discussion.**

473

474 Figure 7

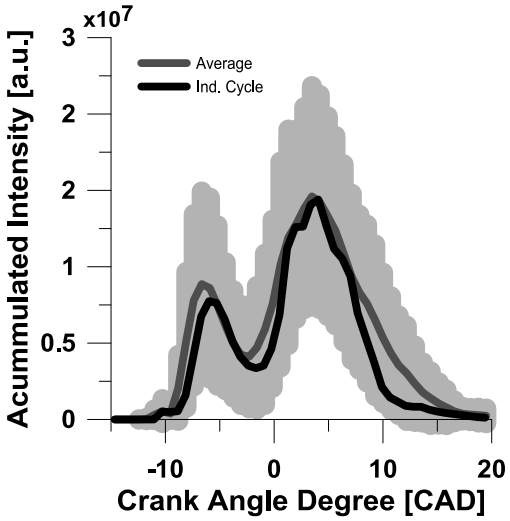


475

476 **Fig. 7 - Flame area dispersion for 30 SACI cycles. The**
477 **shadowed area represents mean Flame area ± std. deviation.**
478 **Thick black curve represents cycle employed on result**
479 **discussion.**

480

481

482

483

484

485 Figure 8

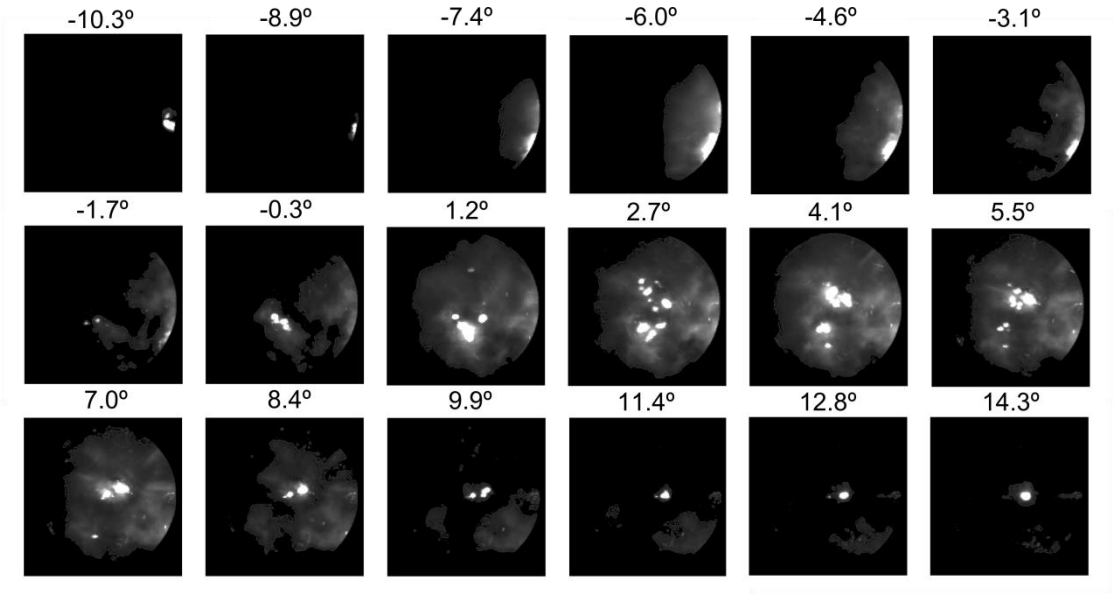


**Fig. 8– Time evolution of natural luminosity inside the combustion chamber.**

Figure 9

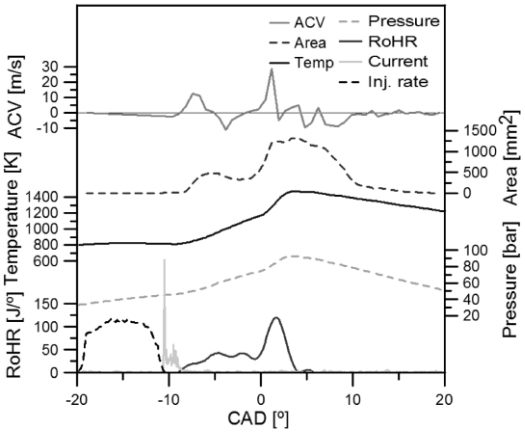


**Fig. 9 – Crankangle evolution of different variables. From top to bottom: image processed variables (ACV and apparent combustion area), in-cylinder pressure analysis (temperature, pressure and hear release rate), injection rate and spark discharge intensity.**

Figure 10

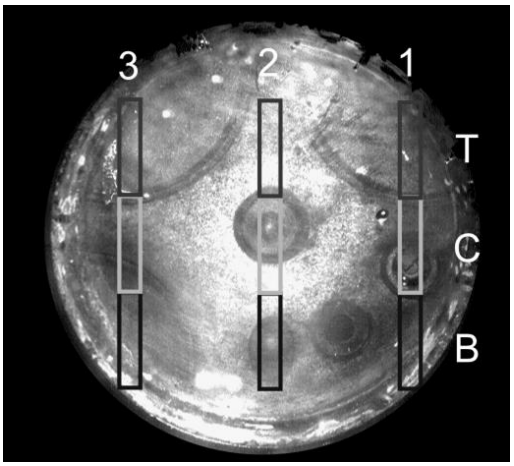


**Fig. 10 – Combustion chamber division for chemiluminescence measurements**

Figure 11

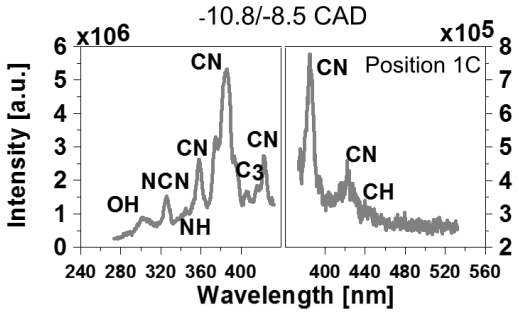


**Fig. 11 – Spectra registered at 1C between -10.8 and -8.5 CAD**

Figure 12

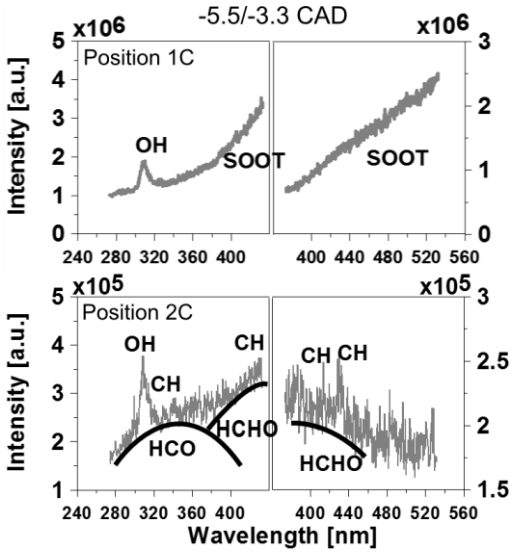


**Fig. 12 – Spectra registered at 1C and 2C between -5.5 and -2.3 CAD**

Figure 13

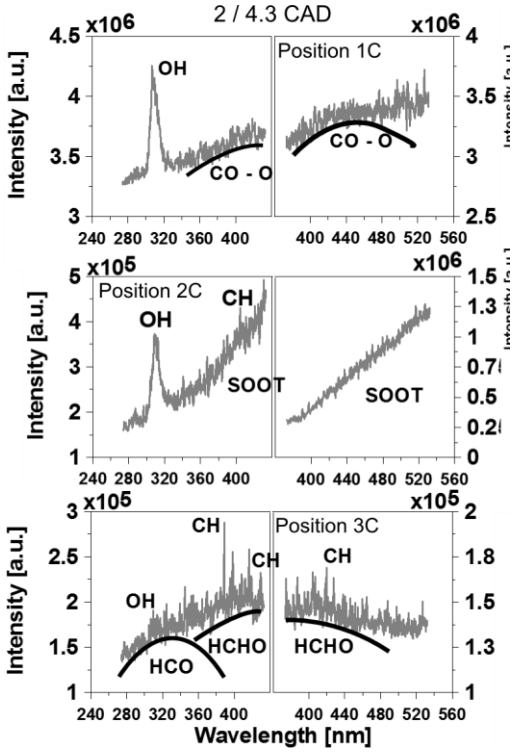


513

514 **Fig. 13 – Spectra registered at 1C, 2C and 3C between 2**
515 **and 4.3 CAD**

516 Figure 14

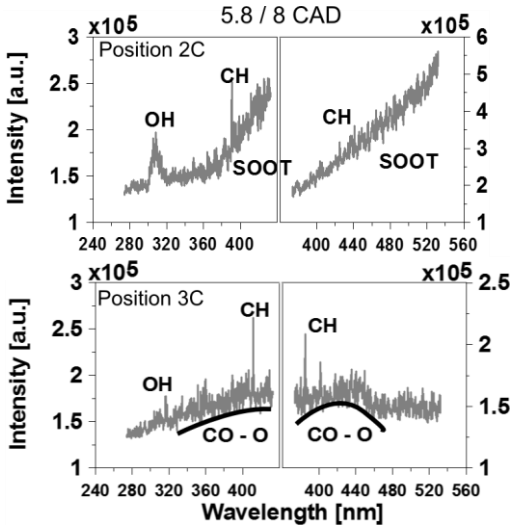


517

518 **Fig. 14 -Spectra registered at 2C and 3C between 5.8 and**
519 **8 CAD**

520

521